**Structural Engineering and Mechanics**, *Vol. 50, No. 2 (2014) 201-214*
DOI: http://dx.doi.org/10.12989/sem.2014.50.2.201 

# Slenderness limit for SSTT-confined HSC column

Ma Chau Khun[a], Abdullah Zawawi Awang[*] and Wahid Omar[b]

*Faculty of Civil Engineering, University Technology Malaysia, Malaysia*

*(Received May 13, 2013, Revised February 7, 2014, Accepted February 25, 2014)*

**Abstract.** Due to the confinement effects, Steel-Straps Tensioning Technique (SSTT) can significantly enhance the strength and ductility of high-strength concrete (HSC) members (Moghaddam *et al.* 2008). However, the enhancement especially in strength may result in slender member and more susceptible to instability (Jiang and Teng 2012a). This instability is particularly significant in HSC member as it inherent the brittle nature of the material (Galano *et al.* 2008). The current slenderness limit expression used in the design is mainly derived from the experiment and analysis results based on Normal strength concrete (NSC) column and therefore the direct application of these slenderness limit expressions to the HSC column is being questioned. Besides, a particular slenderness limit for the SSTT-confined HSC column which incorporated the pre-tensioned force and multilayers effects is not yet available. Hence, an analytical study was carried out in the view of developing a simple equation in order to determine the slenderness limit for HSC column confined with SSTT. Based on the analytical results, it was concluded that the existing slenderness limit expressions used in the design are appropriate for neither HSC columns nor SSTT-confined HSC columns. In this paper, a slenderness limit expression which has incorporated the SSTT-confinement effects is proposed. The proposed expression can also be applied to unconfined HSC columns.

**Keywords:** steel straps; confinement; high-strength concrete; slender column; slenderness limit

## 1. Introduction

Steel-Straps Tensioning Technique (SSTT) has been proven to be an effective means to enhance to load-carrying capacity of High-Strength Concrete (HSC) but most importantly, it can significantly improve the ductility of HSC. This confinement method used low-cost steel-straps which are normally seen in the packaging industry. The steel-straps were pre-tensioned around the column by using the pneumatic tensioner prior to the application of loading. Different from the conventional confining method where confining effect is initiated by the dilation of concrete itself, the pre-tensioned force provides by SSTT can ensure the structure was perfectly confined even before dilation.

In general, a simplified slenderness limit expression is provided in design codes to classify a column into short or slender category. This slenderness limit is particularly important as it is required in the design due to more straight forward design procedure for short column as

*Corresponding author, Senior Lecturer, E-mail: Abdullahzawawi@utm.my
[a]Ph.D. Student, E-mail: machaukhun@gmail.com
[b]Professor, E-mail: drwahid@utm.com.my


http://www.techno-press.org/?journal=sem&subpage=8 ISSN: 1225-4568 (Print), 1598-6217 (Online)

slenderness effect can be ignored. Besides, wrong classifying a slender column as short column can cause catastrophic consequences where overestimation of the column capacity is possible. Therefore, a proper and accurate slenderness limit expression that separates short columns from the slender columns is particularly important in the first step of design. However, a proper slenderness limit for SSTT-confined HSC columns is not yet available and the direct application of the existing slenderness limit expressions of RC columns to SSTT-confined HSC columns is not appropriate. Among the design guidelines for externally confined columns (ISIS 2001, ACI 2008, fib 2001, JSCE 2002, Concrete Society 2004) are all available, only ISIS (2001) provides a slenderness limit expression which is applicable for flexural member without significant bending. It also has been proven in the previous (Mirmiran *et al*. 2001a, Tamuzs *et al*. 2007, Jiang Teng 2012a, Fitzwiliam and Bisby 2012) that confined concrete columns experience greater slenderness effects compared to the unconfined counterparts. The confinement effects can cause an originally short RC column to behave similar to slender column. Hence, the existing slenderness limits proposed by the current design guidelines are not suitable for SSTT-confined HSC column.

In this paper, the development of a simple yet accurate slenderness limit expression for such a column is presented. A parametric study was conducted to investigate all parameters affecting the slenderness limit. The parameters investigated in this paper are eccentricity ratio, normalized eccentricity, depth ratio, steel reinforcement ratio and SSTT-confinement ratio. A simple slenderness limit is then proposed governing all affecting parameters only.

## 2. Theoretical model

The analysis method used is the numerical integration method. Newmark (1943) originally used this method to pin-ended column. In this paper, the column is assumed to be subjected to end eccentricities at both ends. Fig. 1 shows the schematic drawing of the theoretical model. $e_i$ is always the end eccentricity with positive value while $e_s$ can be a negative value. However, the absolute $e_s$ should be anytime smaller than $e_i$. The column is equally segmented into *dL* representing a segment point. Besides, the column cross-section is divided into equally wide horizontal layers. Based on the load-moment-curvature curves of the columns section, the lateral displacement can then be determined by iterative method. The lateral deflection is determined respective to each incremental load and full set of load-deflection curve is drawn.

The capacity of SSTT-confined HSC sections can be calculated if the stress-strain model for such a concrete is known. However, strain gradient exists for column subjected to eccentricity loading and it is general practice to assume that this effect is negligible. In this research, the stress-strain model with confinement effects was used. This model was proposed by Awang (2012). The axial load, *N* and bending moment, *M* is found based on the equations below

$$N = \sum_{i=0}^{n} f_{ci} y_i \, dl + (\sigma_{si} - f_{ci}) A_{si} \tag{1a}$$

$$M = \sum_{i=0}^{n} (f_{ci} y_i \, dl) P_i + (\sigma_{si} - f_{ci})(R - d_{si}) A_{si} \tag{1b}$$

where $y_i$ is the width of *i*-th layer, dl is the thickness of each layer equivalent to 3 mm, $\boldsymbol{\sigma}_{si}$ is the stress of longitudinal steel bar at *i*-th layer, $A_{si}$ is the corresponding cross-sectional area of the longitudinal steel bar, $P_i$ is the moment arm from center point of *i*-th layer to the location of neutral axis, *R* is the radius of column section given by *R=D/2* and $d_{si}$ is the location of longitudinal tensile bar from the extreme concrete fiber as can be seen in Fig. 2.

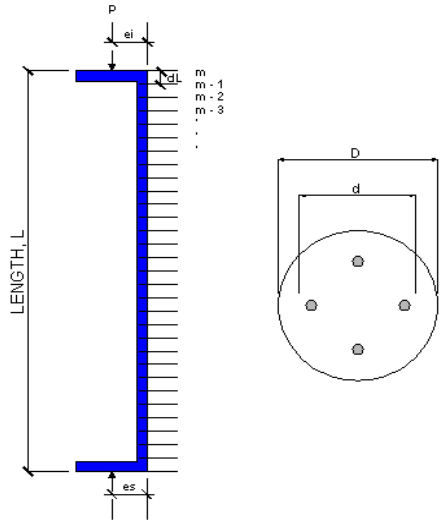


Fig. 1 Schematic of theoretical model

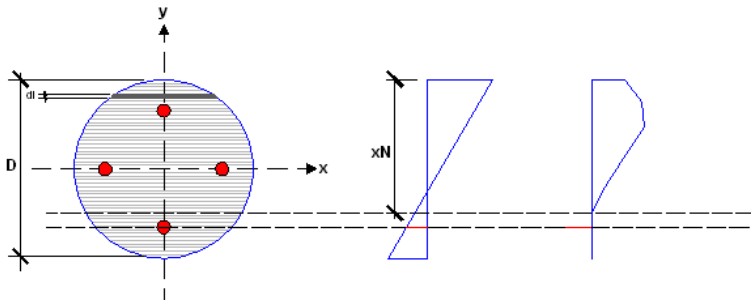


Fig. 2 Strain and stresses over the circular SSTT-confined column

The confined concrete strength can be determined based on the pre-tensioned force and multilayer system of SSTT from Awang (2012)

$$f'_{cc} = f_{co} \times 2.62\left(\rho_s \frac{f_y}{f_{co}}\right)^{0.4} \quad \text{and} \quad \rho_s = \frac{V_s}{V_c} \tag{2d}$$

where

$f_{co}$ = unconfined concrete strength

$\rho_s$ = confining steel volumetric ratio

The peak strain $\varepsilon'_{cc}$ is calculated as below

$$\frac{\varepsilon_{\prime cc}}{\varepsilon_{\prime co}} = 11.60\left(\rho_s \frac{f_y}{f_{co}}\right) \tag{2e}$$

where

$\varepsilon'_{co}$ = concrete axial strain for unconfined concrete strength $f_{co}$

The reference column used in this study is circular with diameter $D$=150 mm. The concrete characteristic cube strength is 60 MPa. 4 steel bars is distributed around the column evenly. The characteristic yield strength of the steel is 460 MPa with elastic modulus, $E_s$=200 GPa.

This analysis equally divided the column section into 50 layers with each thickness of 3 mm. In order to ensures accuracy, the solution is stopped when difference between the resultant load and assumed load exceeded $10^{-6}$ N. The lateral-deflection and curvatures can be related through

$$\delta_{m+1} - 2\delta_m + \delta_{m-1} = -\phi_m \times dl^2 \quad (3)$$

where $\delta_m$ and $\phi_m$ are the lateral displacement and curvature at *m*-th grid point respectively. *m* is the index of grid point

Small increment of the axial load is required to obtain the complete load-deflection curve. It is simple to find the first-order moment for a given axial load as below

$$M_{f,step} = N_{step}\, x\, e_m \quad (4)$$

where $M_{f,\text{step}}$ and $e_m$ are the first-order moment and the eccentricity at the *m*-th point respectively. The second-order moment, $M_{s,\,step}$ can be expressed as

$$M_{s,step} = N_{step}\, x\, \delta_m \quad (5)$$

The final moment can be calculated by:

$$M_{step} = M_{f,step} + M_{s,step} = N_{step} \times (e_m + \delta_m) \quad (6)$$

In this research, the calculation is stopped when the absolute $\delta_m$ value is smaller than $10^{-4}$ mm.

## 3. Verification of the theoretical model

### *3.1 Comparison with HSC column tests*

Comparison was made between the predictions from theoretical model and experimental results. First, Kim's (2007) tests on circular HSC columns are compared. Table 1 shows the detail of Kim. In this experiment test, all specimens were subjected to equal end eccentricities. Since the tested columns were subjected to concentrically loading, a small eccentricity 1 mm was used when analyzing the column in order to lead the column to single curvature bending. $N_u$ and $N_{theo}$ are the test and theoretical axial load capacities of a column respectively. From Table 1, close agreement can be observed between the theoretical predictions and the test results. The largest difference between the theoretical predictions and the test results 1.013.

Test on slender HSC columns performed by Chuang and Kong (1997) were also being compared with the theoretical results. Table 2 shows the properties and the experimental results. It can be observed that the model is accurately predicted the ultimate load of slender column. The

Table 1 Summaries of Kim's (2007) tests

| specimen | *D* (mm) | *l* (mm) | $f_{co}$ (MPa) | $f_y$ (MPa) | $\rho$(%) | *d/D* | $e_i/e_s$ | $e_s/D$ | $N_u$ (kN) | $N_{theo}$ (kN) | $\frac{N_{theo}}{N_u}$ |
|---|---|---|---|---|---|---|---|---|---|---|---|
| 10C1$^3/_8$-ρ2.5 | 300 | 1000 | 55 | 435 | 2.5 | 0.96 | 1 | 0 | 6387 | 6355 | 1.005 |
| A10C1$^3/_4$-ρ2.5 | 300 | 1000 | 80 | 435 | 2.5 | 0.96 | 1 | 0 | 5564 | 5490 | 1.013 |
| 14C1- ρ2.5 | 300 | 1000 | 111 | 435 | 2.5 | 0.96 | 1 | 0 | 8896 | 9002 | 0.988 |
| 18C1$^3/_8$-ρ2 | 225 | 900 | 104 | 435 | 2 | 0.944 | 1 | 0 | 4688 | 4685 | 1.001 |

Table 2 Summaries of Chuang and Kong's (1997) tests

| specimen | $H$ (mm) | $B$ (mm) | $l$ (mm) | $f_{co}$ (MPa) | $f_y$ (MPa) | $d/D$ | $e_s/D$ | $N_u$ (kN) | $N_{theo}$ (kN) | $\frac{N_{theo}}{N_u}$ | $\boldsymbol{\delta}_{exp}$ (mm) | $\boldsymbol{\delta}_{theo}$ (mm) | $\frac{\delta_{exp}}{\delta_{theo}}$ |
|---|---|---|---|---|---|---|---|---|---|---|---|---|---|
| HB-17-0.25 | 200 | 300 | 3400 | 96.2 | 531 | 0.1 | 0.25 | 1800 | 1712 | 1.051 | 35 | 31 | 1.129 |
| HB-18-0.25 | 200 | 300 | 3600 | 94.8 | 531 | 0.1 | 0.25 | 1477 | 1453 | 1.017 | 30 | 35 | 0.857 |
| HB-19-0.25 | 200 | 300 | 3800 | 95.4 | 531 | 0.1 | 0.25 | 1573 | 1391 | 1.131 | 15 | 37 | 0.405 |
| HB-17-0.5 | 200 | 300 | 3400 | 94.1 | 531 | 0.1 | 0.5 | 706 | 770 | 0.917 | 34 | 38 | 0.895 |
| HB-18-0.5 | 200 | 300 | 3600 | 95.9 | 531 | 0.1 | 0.5 | 647 | 660 | 0.98 | 40 | 44 | 0.909 |
| HB-19-0.5 | 200 | 300 | 3800 | 96.1 | 531 | 0.1 | 0.5 | 607 | 632 | 0.96 | 39 | 47 | 0.83 |

Table 3 Xu's (2012) tests

| specimen | $H$ (mm) | $B$ (mm) | $l$ (mm) | $\rho$(%) | $d/D$ | $e_s/D$ | $N_u$ (kN) | $N_{theo}$ (kN) | $\frac{N_{theo}}{N_u}$ | $\boldsymbol{\delta}_{exp}$ (mm) | $\boldsymbol{\delta}_{theo}$ (mm) | $\frac{\delta_{exp}}{\delta_{theo}}$ |
|---|---|---|---|---|---|---|---|---|---|---|---|---|
| CS-0 | 150 | 150 | 800 | 2 | 0.87 | 0 | 1112.9 | 1150 | 0.968 | 2.13 | 1.89 | 1.126 |
| CS-15 | 150 | 150 | 800 | 2 | 0.87 | 0.1 | 917.1 | 850 | 1.079 | 19 | 18.65 | 1.019 |
| CS-25 | 150 | 150 | 800 | 2 | 0.87 | 0.17 | 778.1 | 710 | 1.096 | 56 | 35 | 1.6 |

maximum deflections of the tested specimens were also compared with the predicted deflections. It is worth noting that for the HB-L/h-0.25 column series, the reported maximum deflections reduced as the column slenderness increases. This phenomenon was not explained by the author but obviously, the findings are contradicted with the results reported by the others. The predicted results show that the maximum deflection increases as the slenderness increases. This results in the large difference between the experimental and theoretical results for HB-19-0.25. However, as can be seen for HB-L/H-0.5 column series, the predicted results are in good agreement with the experimental results as in this series of column the maximum deflection increases as the column slenderness increases.

### *3.2 Comparison with SSTT-confined column*

The theoretical and experimental results of Steel-straps confined columns tested by Xu (2012) were compared in Table 3. The columns were square in cross-section with 150 mm sides and 800 mm height. Four longitudinal reinforcements with 12 mm were provided. For stirrups, 6mm plain bar with 120 mm spacing were provided. The yield strength for longitudinal reinforcement and plain bar were 500 MPa and 250 MPa respectively. The concrete used has the concrete compressive strength of 32 Mpa and the cover was fixed to 20 mm. In the test, the steel-straps with a nominal thickness of 0.78 mm and a width of 19.1 mm were used. The spacing of the steel-straps was fixed to 30 mm. It should be noted that all specimens in this test were circularized to avoid confining strength loss due to sharp corner. Segmental circular concrete covers with corner radius of 20 mm were bonded on the surface of the column. The properties of the specimens were listed in Table 3. The only parameter varies in the testing is the eccentricity of loading. For column CS-0, since the tested specimen was loaded concentrically, hence no load- deflection curve was reported. Meanwhile, the load-deflection curves of Column CS-15 and CS-25 were compared with

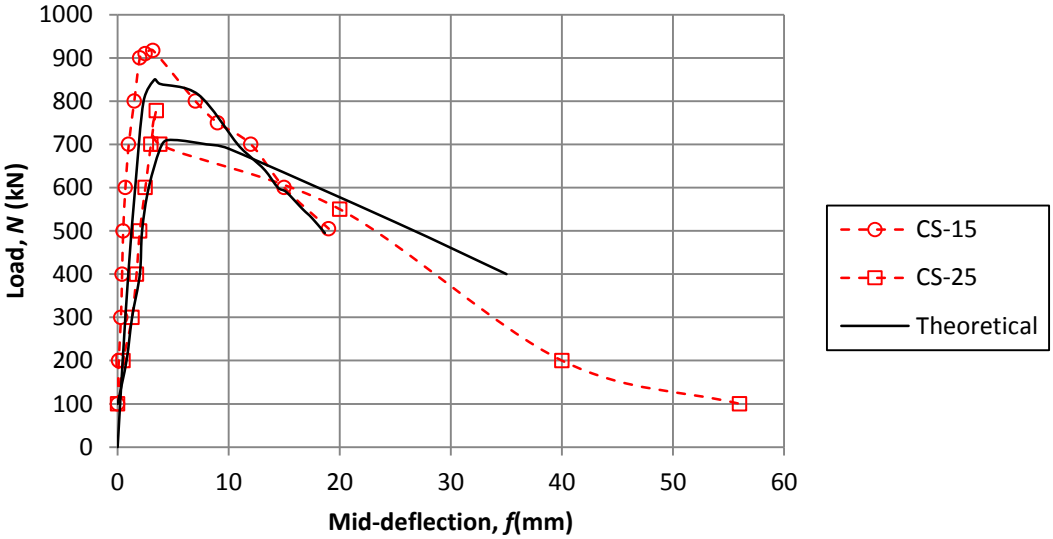


Fig. 3 Load-deflection curves of Xu's (2012) test

the theoretical load-deflection curves in Fig. 3. The predicted load-deflection curves show good agreement with the experimental results. The predicted ultimate load for both specimens is slightly conservative compared to the experimental results. For Column CS-15, the predicted maximum deflection is perfectly matched with the reported maximum deflection. However, as can be seen in Column CS-25, the maximum deflection estimated by the theoretical model is less than the tested results. However, the deflection after 85% post peak of ultimate load shows good agreement with the tested results. This is particularly important since the deflection at 85% after post-peak load is widely adopted to measure the displacement ductility of slender column. Besides, as has been reported by Awang *et al*. (2012), the proposed stress-strain model used in the theoretical model herein is validated for both circular NSC and HSC. However, as can be seen in Figure 3, this stress-strain model is sufficiently accurate in generating the load-deflection curves for square cross-section column, provided that the column is circularized to ensure perfect confinement.

## 4. Results and discussions

### *4.1 Results for HSC columns*

Fig. 4 shows the numerical results of the effect governed by the eccentricity ratio. Each curve represents the slenderness limit at particular end eccentricities with different eccentricities ratio. It is clearly seen that, the slenderness limit tend to decrease with the increase of eccentricity ratio. This can be explained as column bent in single curvature always exposed to greatest slenderness effect. It is observed in Fig. 3 that the reduction of slenderness limit is more significant in the case of large normalized eccentricity. However, the effect of the normalized eccentricity was ignored in the current design guidelines (ACI-318 2005). Since the influence of the normalized eccentricity is pronounced, this effect must be included in the slenderness limit design. The slenderness limit

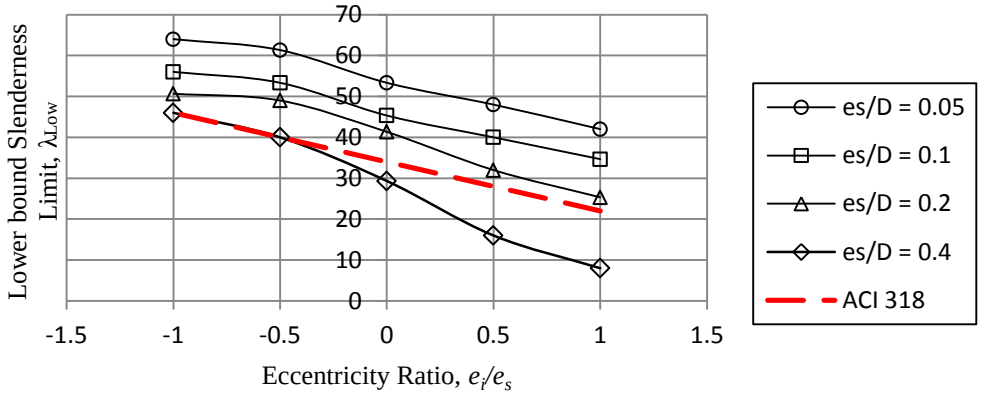


Fig. 4 Effect of eccentricity ratio

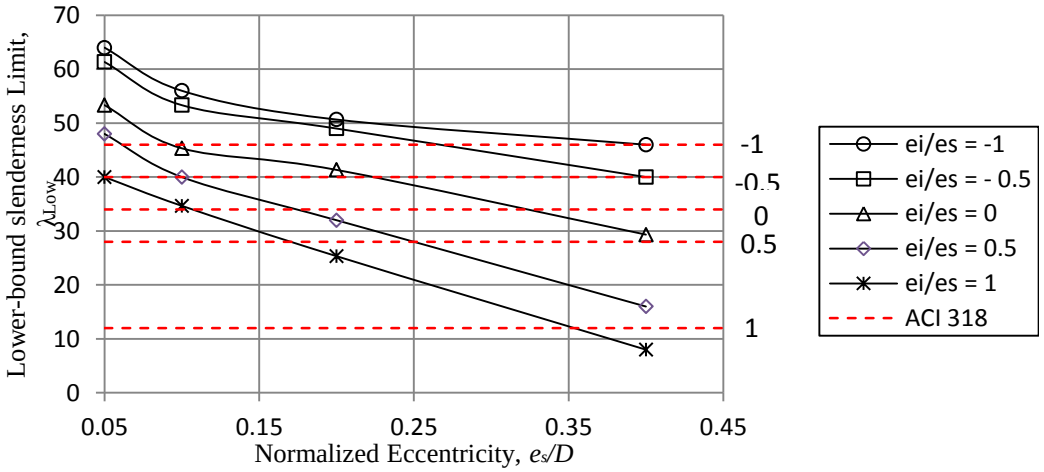


Fig. 5 Effect of normalized eccentricity

decreased rapidly with the increment of normalized eccentricity, as in Fig. 5. This can be explained as the load capacity of HSC column reduces with the increases of normalized eccentricity. It is observed that the slenderness HSC column experienced larger load capacity reduction when in the case of large eccentricity ratio. As discussed previously, column with large eccentricity ratio always expose to largest slenderness effect, as the normalized eccentricity increased, this effect is amplified.

Fig. 6 shows the effect of the concrete cover thickness to the slenderness limit. To this extent, the concrete cover thickness is represented as normalized depth ratio, *d/D* in this paper. It was reported by past research (Jiang and Teng 2012b), that the concrete cover has insignificant influence the stability of a slender column. Thick concrete cover can prevent the premature buckling of the longitudinal steel bar and also provide certain degree of confinement to the concrete core. However, as can be seen in the Fig. 6, the effect of concrete cover thickness is insignificant. Hence, this effect can be ignored in order to develop a simple slenderness limit expression for HSC column.

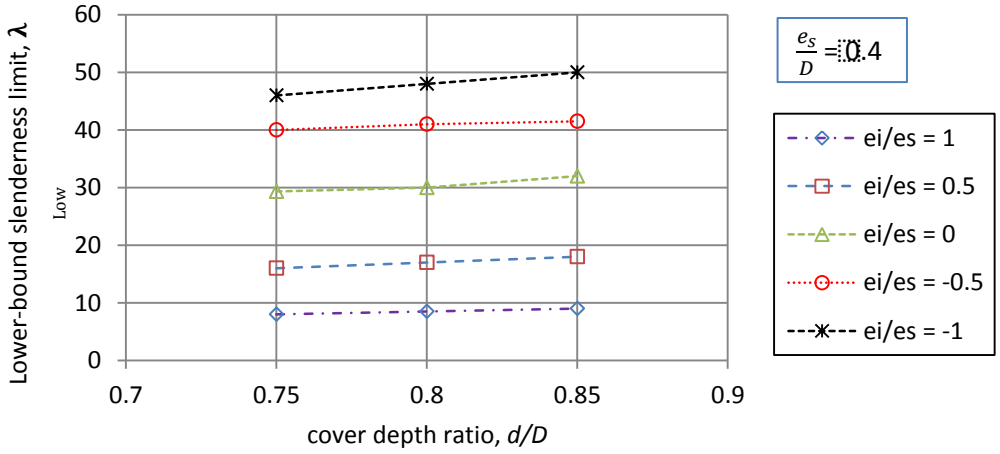


Fig. 6 Effect of depth ratio

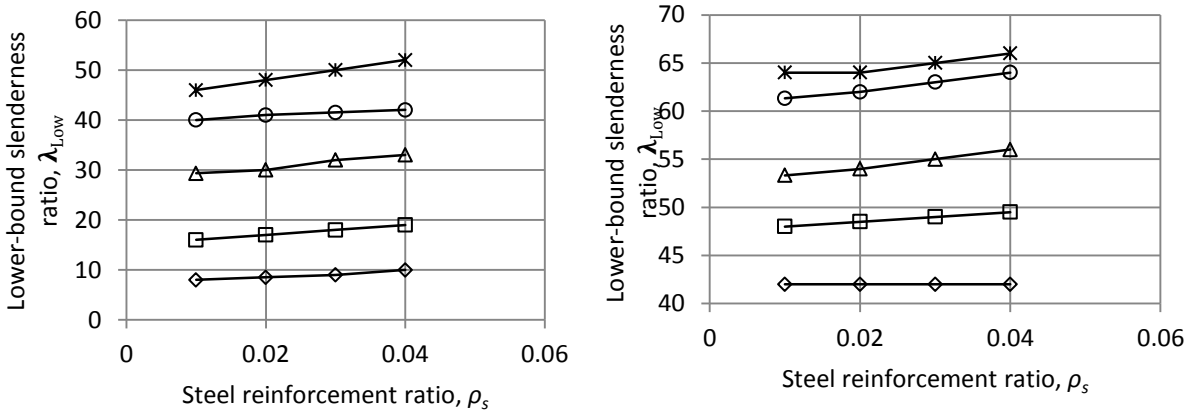


(a) $e_s/D$=0.05 (b) $e_s/D$=0.4

Fig. 7 Effect of steel reinforcement ratio

Fig. 7 shows the effect of steel reinforcement ratio to the slenderness limit. With higher steel reinforcement ratio, slender column was reported to have better stability. In the examination of this effect to the slenderness limit of HSC, numerical analysis was carried out to study the steel reinforcement ratio ranging from 0.01 indicating low reinforcement ratio to 0.05 indicating high reinforcement ratio. It should be noted that the numerical results are based on the $e_2/D$=0.05 and $e_2/D$=0.04 only since the results for the intermediate normalized eccentricities are almost similar. It can be clearly seen that the effect of steel reinforcement ratio to the slenderness limit is also insignificant.

The results indicate that the eccentricity ratio and the normalized eccentricity have most significant effects on the slenderness limit of short HSC columns. They should be taken into consideration when developing a design expression for the slenderness limit of SSTT-confined HSC columns. Meanwhile, the effects of depth ratio and steel reinforcement ratio should be

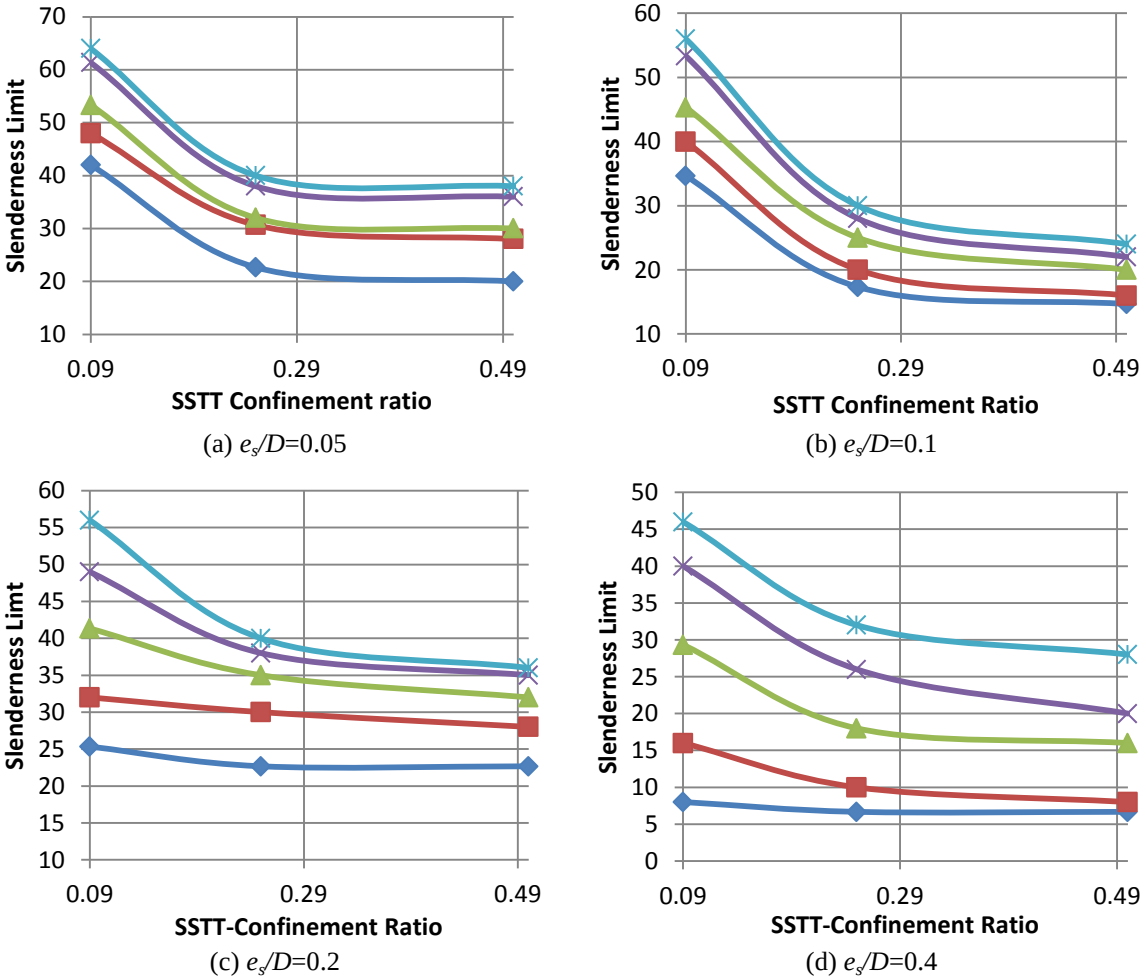


(a) $e_s/D$=0.05 (b) $e_s/D$=0.1

(c) $e_s/D$=0.2 (d) $e_s/D$=0.4

Fig. 8 Effect of SSTT-confinement ratio, $\rho_v$

neglected to keep the design equation as simple as possible.

### *4.2 Results for SSTT-confined HSC columns*

In determining the effect of SSTT confinement, the effects of pre-tensioned force and multilayers system has to be considered. However, in the view to suggest an accurate yet simple design expression, these effects were grouped in one parameter: SSTT-confinement volumetric ratio, $\rho_v$. The SSTT-confinement volumetric ratio, $\rho_v = \frac{V_s.f_y}{V_c.f_{co}}$. Figure 8 show the effect of SSTT-confinement volumetric ratio, $\rho_v$. As stated earlier, SSTT volumetric ratio, $\rho_v$=0 represents the case of unconfined column. Fig. 8 present sub-figures with respect to different axial load level. It can be clearly seen that, the confinement start to have effects when the SSTT-confinement ratio, $\rho_v \geq 0.09$. A general trend can be extracted from Fig. 8, which is the slenderness limit decreases as the SSTT-confinement volumetric ratio increases. However, the reduction in the slenderness limit can be

observed when the normalized eccentricity is increased as in Fig. 8(c) and (d). It is clearly seen that in Fig. 8, the uppermost curve shown in Fig. 8(a) has the sharpest slope. This indicating smaller eccentricity ratio combined with higher load has the most significant effect of the SSTT-confinement volumetric ratio, $\rho_v$.

## 5. The development of slenderness limit

To simplify the design of SSTT-confined HSC columns, the proposed slenderness limit are established as a function of $\rho_s$, $\frac{e_i}{e_s}$ and $\frac{e_s}{D}$. The function was established by nonlinear regression analysis. The developed relation with disregard of the effect of SSTT-confinement is as follow

$$\boldsymbol{\lambda}_{\text{lim}} = 50\,\frac{e_s}{D}\left(1 - \frac{e_i}{e_s}\right) + 24\left(1.2 - \frac{e_s}{D}\right)^4 \tag{7}$$

Eq. (7) is the slenderness limit expression for HSC columns with the absence of SSTT-confinement volumetric ratio. ACI-318 (2005) proposed a slenderness limit for NSC column as below

$$\boldsymbol{\lambda}_{\text{lim}} = 34\text{-}12\,\frac{M_1}{M_2} \tag{8}$$

Eq. (8) considers the effects of eccentricity, but the $e_s/D$ is fixed at 0.2. When the Eq. (7) is inserted with the value $\frac{e_s}{D} = 0.2$ , it reduces to $\boldsymbol{\lambda}_{\text{lim}} = 34 - 16\frac{e_i}{e_s}$. This equation is similar but more conservative than Eq. (8). Fig. 8 shows the performance of Eq. (8). The prediction of the proposed expression shows good agreement with the numerical results. As can be seen in Fig. 9, the prediction of HSC column slenderness limit by using either ACI expression or Jiang and Teng's expression cannot captured the behavior accurately. This is mainly due to the differences of material behavior between HSC and NSC. The direct application of the current design guidelines can led to incorrect estimation for slenderness limit of HSC column.

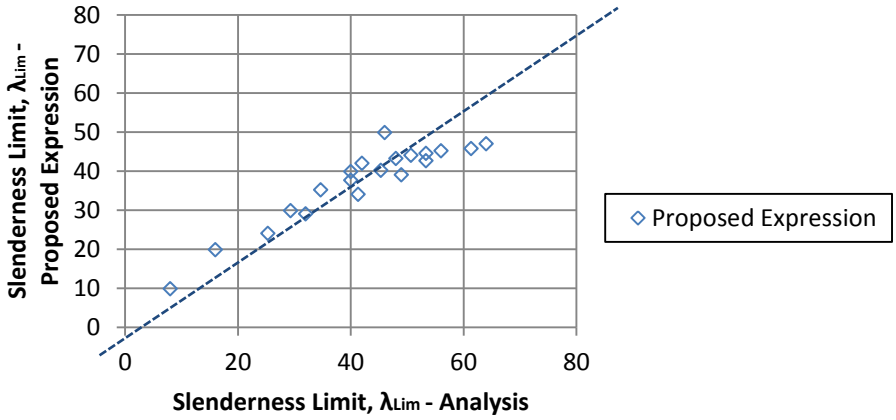


(a) Proposed expression vs Results of analysis

Fig. 9 Performance of the proposed equation for HSC columns

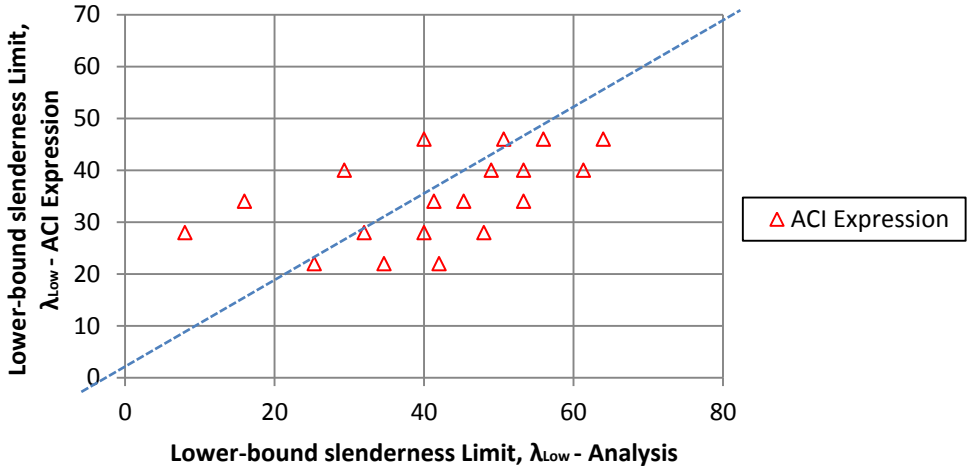


(b) ACI expression vs Results of analysis

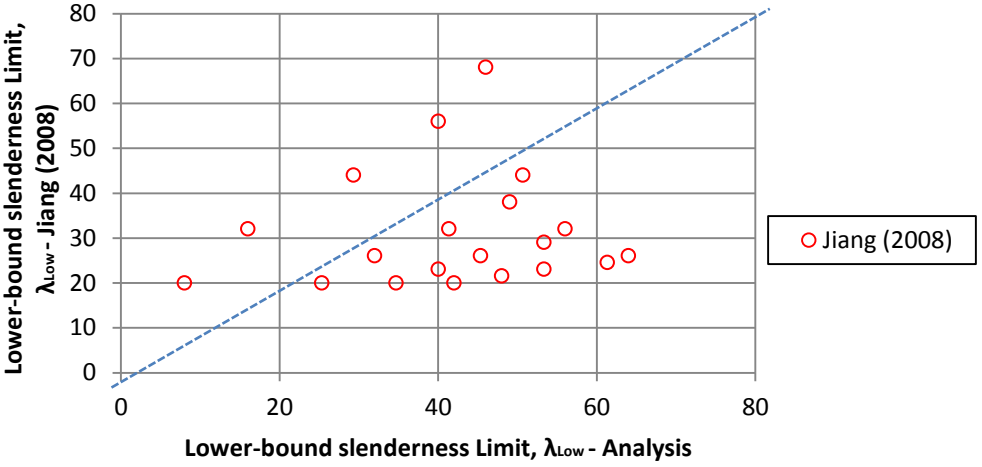


(c) Jiang and Teng expression vs Results of analysis

Fig. 9 Continued

Based on careful interpretation, slenderness limit for SSTT-confined HSC columns can be written as follow

$$\boldsymbol{\lambda}_{\text{lim}} = \frac{50\frac{e_s}{D}\left(1-\frac{e_i}{e_s}\right)+24\left(1.2-\frac{e_s}{D}\right)^4}{6\rho_v-5.7{\rho_v}^2+0.6} \tag{9}$$

The numerator considers the effects of eccentricity ratio and normalized eccentricity, meanwhile the denominator considers the effect of SSTT-confinement volumetric ratio. The performances of the proposed slenderness limit expression are compared with the numerical results as shown in dashed line in Fig. 10. It can be seen that the Eq. (9) can perfectly capture the variation of the slenderness limit of SSTT-confined HSC column.

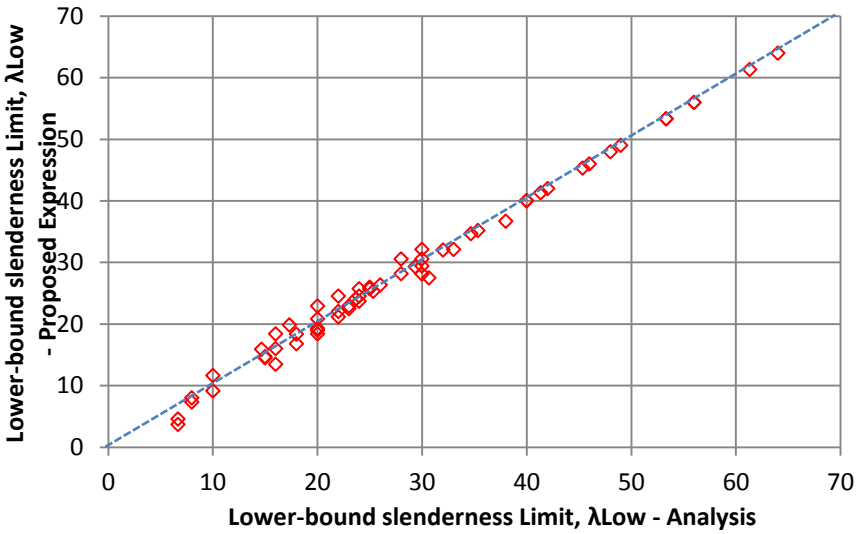


Fig. 10 Performance of proposed expression (Eq. (9))

In summary, the Eq. (9) possesses a simpler form, but sufficiently accurate to define the slenderness limit for SSTT-confined HSC columns.

## 6. Conclusions

A slenderness limit which is suitable for HSC column and SSTT-confined HSC column is proposed for design use. An analysis was conducted to examine various parameters by using the theoretical model as presented in the previous section. The results were interpreted carefully and the slenderness limit of SSTT-confined HSC columns is proposed. Conclusions as follow were drawn:

(i) SSTT-confinement can introduce more pronounce slenderness effect. This is mainly due to steel-straps confinement increased the axial load capacity of HSC columns significantly, but very little increment on the flexural rigidity of the section.

(ii) Two parameters that have the most significant effect on the slenderness limit of HSC and SSTT-confined HSC columns namely the eccentricity ratio and normalized eccentricity. Meanwhile the other parameters such as the reinforcement ratio and depth ratio have only negligible effects on the behavior of SSTT-confined HSC columns.

(iii) A slenderness limit which is suitable for HSC column and SSTT-confined HSC column is proposed herein. The proposed expression aims at greater simplicity with sacrifice of a certain degree of accuracy so that it can be use conveniently in the design of SSTT- confined HSC columns.

## References

Awang, A.Z (2013), “Stress-strain behavior of high-strength concrete with lateral pre-tensioning

confinement", Ph.D. Dissertation, Universiti Teknologi Malaysia, Malaysia.
American Concrete Institue (ACI) (2008), "Design and construction of externally bonded FRP system for strengthening concrete structures", ACI 440.2R-08, American Concrete Institute.
Chuang, P.H. and Kong, F.K (1997), "Large-scale tests on slender, reinforced concrete columns", *Struct. Eng.*, **75**(23-24), 410-416.
Concrete Society (2004), "Design guidance for strengthening concrete structures with fibre composite material", 2nd Edition, Concrete Society Technical Report No. 55, Crowthorne, Berkshire, UK.
fib (2001), "Externally bonded FRP reinforcement for RC structures", The International Federation for Structural Concrete, Lausanne, Switzerland.
Fitzwilliam, J. and Bisby, L.A. (2012), "Slenderness effects on circular CFRP-wrapped reinforced concrete columns", *J. Compos. Construc.*, **14**(3), 280-288.
Galano, L. and Vignoli, A. (2008), "Strength and ductility of HSC and SCC slender columns subjected to short-term eccentric load", *ACI Struct. J.*, **105**(3), 259-69.
Jiang, T. (2008), "FRP-confined RC columns: analysis, behavior and design", Ph.D Dissertation, Hong Kong Polytechnic University, Hong Kong, China.
Jiang, T. and Teng, J.G. (2012a), "Slenderness limit for short FRP-confined circular RC columns", *J. Compos. Construct.*, **16**(6), 650 -660.
Jiang, T. and Teng, J.G. (2012b), "Behavior and design of slender FRP-confined circular RC columns", *J. Compos. Construct.*, doi: 10.1061/(ASCE)CC.1943-5614.0000333.
Kim, S.J. (2008), "Behavior of high-strength concrete columns", Ph.D Dissertation, North Carolina State University, Raleigh, North Carolina.
Mirmiran, A., Shahawy, M. and Beitleman, T. (2001a), "Slenderness limit for hybrid FRP-concrete columns", *Journal of Composites for Construction*, **5**(1), 26-34.
Moghaddam, H., Pilakoutas, K., Samadi, M. and Mohebbi., S. (2008), "Strength and ductility of concrete member confined by external post-tensioned strips", *The 4th National Conference on Civil Engineering, University of Tehran*, Tehran.
Newmark, N.M. (1943), "Numerical procedure for computing deflections, moments, and buckling loads", *ASCE Tran.*, **108**, 1161-1234.
Tamuzs, V., Tepfers, R., Zile, E. and Valdmanis, V. (2007), "Stability of round concrete columns confined by composite wrappings", *Mech. Compos. Mater.*, **45**(3), 191-202.
Xu, L. (2012), "Shape modification of square reinforced concrete columns confined with fibre-reinforced polymer and steel straps", Master of Engineering (Research) Dissertation, University of Wollongong.

## Notations

The following symbols are used in this paper:
$A_{si}$ = corresponding cross-sectional area of longitudinal steel bar
$A_{conc}$ = total cross-sectional area of column
$A_{st}$ = total cross-sectional area of longitudinal bars
$D$ = diameter of column section
$dl$ = thickness of each layer of discretized column section
$dL$ = length of column segmented unit
$d_{si}$ = location of longitudinal tensile bar from the extreme concrete fiber
$e$ = load eccentricities
$e_m$ = load eccentricities at a given column grid-point
$e_i$ = column end eccentricities which always has absolute positive value
$e_s$ = column end eccentricities which can be either positive or negative value
$E_c$ = tangent modulus of elasticity of concrete

$E'_{sec}$= secant modulus of confined concrete at peak stress
$E_s$ = steel elastic modulus
$\varepsilon_{co}$ = Ultimate strain of HSC
$\varepsilon'_{cc}$ = confined concrete's peak strain
$\varepsilon_s$ = strain of steel
$\varepsilon_y$ = yield strain of steel
$\varepsilon_{ci}$ = concrete strain
$\varepsilon_{cc}$ = axial compressive strain of concrete
$f_{ci}$ = concrete stress at a given strain
$f_{co}$ = concrete compressive strength
$f_y$ = yield strength of steel
$f_{l,s}$ = steel straps confinement efficiency based on Lei's model (2012)
$k_{ss}$ = efficiency factor for steel-straps confinement
$L$ = length of column
$M_{step}$ = bending moment at successively incremental loading steps
$M_{f,\,step}$ = first-order moment at a given load step
$M_{s,\,step}$ = second-order moment at a given load step
$N_{step}$ = axial load at successively incremental loading steps
$N_{ult}$ = ultimate load capacity of column under concentric load
$N_{u,\,test}$ = ultimate load from experimental test
$N_{u,\,theo}$ = ultimate load from theoretical analysis
$R$ = radius of column section
$s$ = clear spacing of steel straps
$t_s$ = thickness of steel straps
$V_s$ = volume of SSTT-confinement
$V_c$ = volume of concrete
$x$ = ratio of axial compressive strain to concrete peak strain
$xN$ = neutral axis
$y_i$ = width of *i-th* layer
$\rho_s$ = sstt-confinement volumetric ratio
$\rho$ = internal reinforcement ratio
$\delta_m$ = lateral deflection at a given column grid-point
$\delta$ = lateral deflection
ø = curvature
$\sigma_{si}$ = stress of longitudinal bar at *i-th* layer